

# Capillary-gravity solitary waves with damped oscillations

Frédéric Dias and Gérard Iooss

*Institut Non-Linéaire de Nice – UMR CNRS 129, Université de Nice Sophia-Antipolis, Faculté des Sciences,  
06108 Nice cedex 2, France*

Received 11 May 1992

Revised manuscript received 24 November 1992

Accepted 28 December 1992

Communicated by A.C. Newell

Capillary-gravity solitary waves with damped oscillations are studied analytically. The analysis follows the work of Iooss and Kirchgässner who proved that these waves exist for all values of the Froude number smaller than one. The water-wave problem is reduced to a system of ordinary differential equations by using the center manifold theorem. The normal form of this reduced system can be obtained and a good approximation to these waves for small amplitude is constructed. The limit as the water depth becomes infinite is considered as a special case. A comparison with existing numerical results is made for small-amplitude waves.

## 1. Introduction

This paper deals with capillary-gravity solitary waves with damped oscillations in their tail. Kawahara [1], Hunter and Vanden-Broeck [2], and Zufiria [3] have already computed such waves as solutions of a generalized Korteweg–de Vries equation which includes a fifth-order derivative term and is valid in a neighborhood of the critical values  $\lambda = 1$  and  $b = \frac{1}{3}$  (see (1.1) and (1.2) for the definitions of  $\lambda$  and  $b$ ). Hunter and Vanden-Broeck [2], in addition, also used an integrodifferential-equation formulation to compute similar waves for the full equations. Longuet-Higgins [4] computed depression waves based on the full equations for the water-wave problem in infinite depth. Iooss and Kirchgässner [5] proved the existence of such capillary-gravity solitary waves with damped oscillations for the full equations in water of finite depth for all values of the Froude number smaller than one. Vanden-Broeck and Dias [6] computed numerically elevation and depression waves in water of infinite depth, the results for depression waves extending the calculations by Longuet-Higgins [4].

In order to understand the origin of these waves, it is helpful to go back to the classical problem of water waves when both the effects of gravity and surface tension are included. The waves considered in this paper are assumed to travel at a constant velocity  $c$  on water of finite depth  $h$ . These waves can be characterized by the two dimensionless numbers

$$\lambda = \frac{gh}{c^2} \tag{1.1}$$

and

$$b = \frac{T}{\rho h c^2}, \tag{1.2}$$

where  $\rho$  denotes the density of water,  $g$  the acceleration due to gravity and  $T$  the coefficient of surface tension. The number  $\lambda$  is the inverse of the square of the Froude number and  $b$  is the Bond number.

The dispersion relation for linearized capillary-gravity progressive waves with dimensionless wavenumber  $\kappa = Kh$  can be written as

$$D(\kappa, \lambda, b) = (\lambda + b\kappa^2) \tanh \kappa - \kappa = 0. \quad (1.3)$$

For all values of  $b$  and  $\lambda$ ,  $\kappa = 0$  is a root of (1.3) but it does not play a role unless  $\lambda = 1$ . Moreover, if  $\kappa$  satisfies (1.3), so does  $-\kappa$ . Therefore, we concentrate on the positive roots  $\kappa$  of the dispersion relation. Depending on the values of  $b$  and  $\lambda$ , eq. (1.3) can have zero, one or two positive roots. The corresponding regions in the parameter space  $(b, \lambda)$  are shown in fig. 1. Along the curve  $\lambda = 1$ ,  $b > \frac{1}{3}$ , there is a transition from one root to zero root (see fig. 2a). A family of solitary depression waves bifurcates from a uniform flow. Their existence has been proved by Amick and Kirchgässner [7] and by Sachs [8]. These waves have been computed numerically by Hunter and Vanden-Broeck [2]. A good approximation to these waves is given by the solitary-wave solution of the Korteweg-de Vries equation

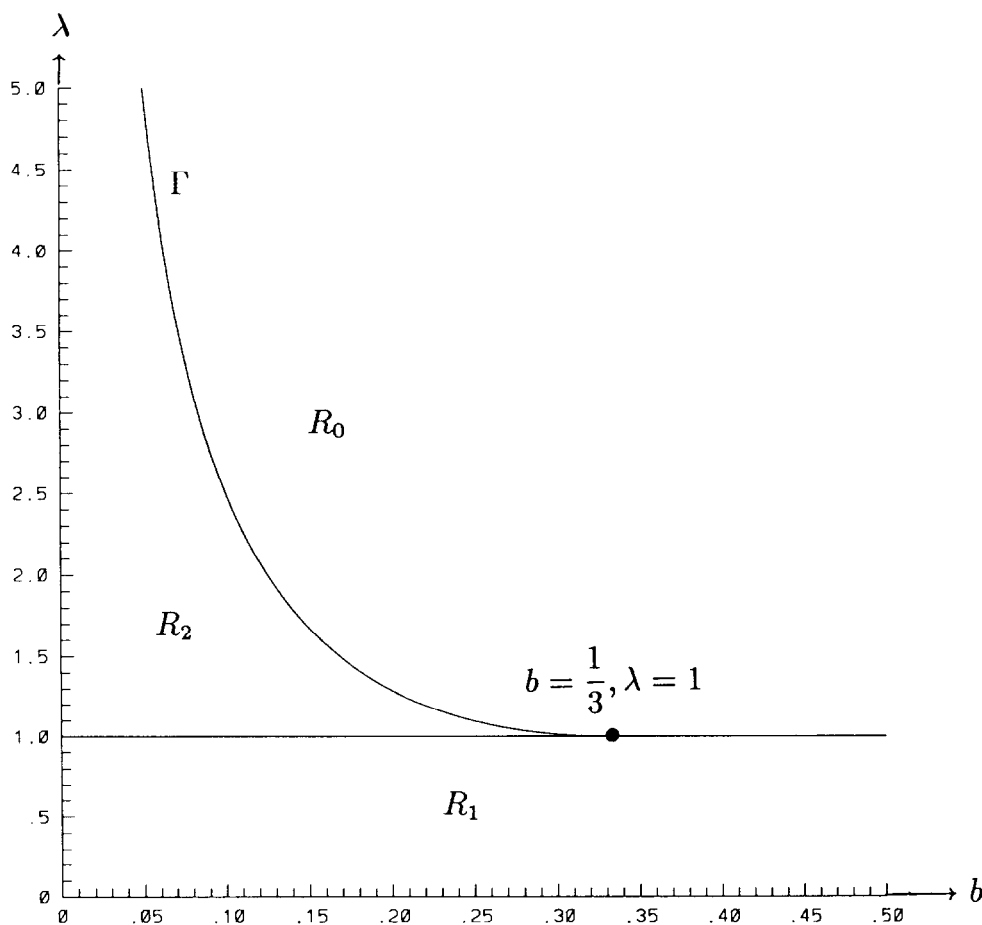


Fig. 1. Regions in the  $(b, \lambda)$ -plane where the dispersion relation has zero ( $R_0$ ), one ( $R_1$ ) or two positive roots ( $R_2$ ).

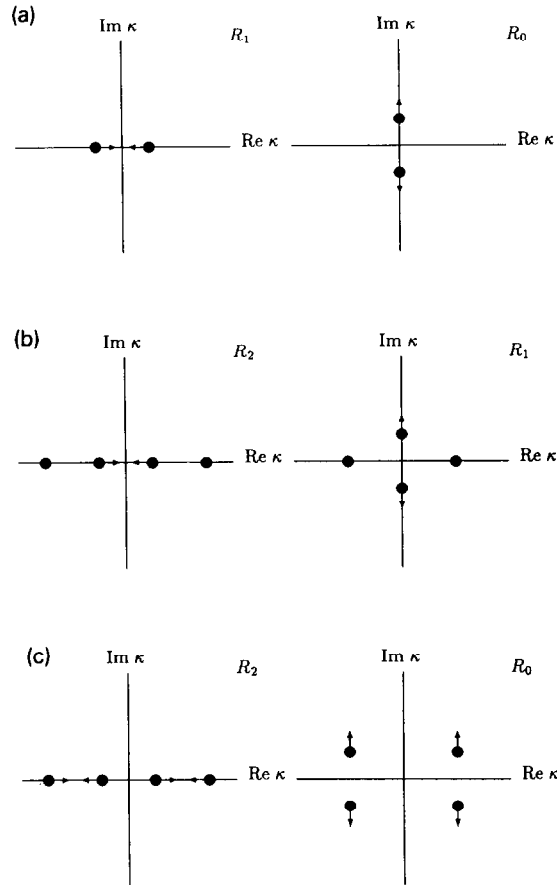


Fig. 2. Transition regions for the positive roots  $\kappa$  of the dispersion relation (1.3). (a) shows the transition from one to zero root, (b) from two to one, and (c) from two to zero. The regions  $R_0$ ,  $R_1$ ,  $R_2$  are shown in fig. 1.

for  $b > \frac{1}{3}$ . Along the curve  $\lambda = 1$ ,  $b < \frac{1}{3}$ , there is a transition from two roots to one root (see fig. 2b) and more complex mathematical phenomena occur. In particular, Iooss and Kirchgässner [9], Beale [10], and Sun [11] have proved existence results for generalized solitary waves consisting of a single crest plus a train of periodic waves of much smaller amplitude which persists at infinity. A good approximation to the shape of the single crest is given by the solitary-wave solution of the Korteweg–de Vries equation for  $b < \frac{1}{3}$ . Numerical computations by Vanden-Broeck [12] have produced particular waves for which the amplitude of the small oscillations is zero within numerical accuracy. Lombardi [13] mathematically proved that the amplitude can be extremely small. But whether or not the amplitude at infinity can be exactly zero remains an open problem.

The curve denoted by  $\Gamma$  in fig. 1 corresponds to the transition from two roots to zero root (see fig. 2c). On  $\Gamma$ , the two positive roots merge into a double root. The curve  $\Gamma$  is obtained when both eq. (1.3) and the following equation

$$\frac{\partial D}{\partial \kappa} = 2b\kappa \tanh \kappa + (\lambda + b\kappa^2)(1 - \tanh^2 \kappa) - 1 = 0 \quad (1.4)$$

are satisfied. A physical interpretation can be given for the curve  $\Gamma$ : it consists of the points  $(b, \lambda)$  for

which the phase velocity  $c$  is equal to the group velocity  $c_g$ . Recall that  $c$  is given by the dispersion relation (1.3) which can be rewritten as

$$c^2 = \left( \frac{gh}{\kappa} + \frac{T\kappa}{\rho h} \right) \tanh \kappa ,$$

and that  $c_g$  is given by

$$c_g = \frac{\partial(c\kappa)}{\partial\kappa} = c + \kappa \frac{\partial c}{\partial\kappa} .$$

In parametric form,  $\Gamma$  consists of the points  $(b, \lambda)$  given by

$$b = \frac{1}{2\kappa \sinh^2 \kappa} (\sinh \kappa \cosh \kappa - \kappa) , \quad (1.5)$$

$$\lambda = \frac{\kappa}{2 \sinh^2 \kappa} (\sinh \kappa \cosh \kappa + \kappa) , \quad (1.6)$$

where  $\kappa$  runs from zero to infinity. In the limit as  $\kappa$  approaches zero,

$$b \sim \frac{1}{3} - \frac{2\kappa^2}{45} , \quad \lambda \sim 1 + \frac{\kappa^4}{45} .$$

In the limit as  $\kappa$  approaches infinity,

$$b \sim \frac{1}{2\kappa} , \quad \lambda \sim \frac{\kappa}{2} .$$

The dimensionless number  $b\lambda$  plays an important role in the analysis. It can be shown that  $b\lambda$  decreases monotonically from  $\frac{1}{3}$  to  $\frac{1}{4}$  as  $\kappa$  increases from zero to infinity. Iooss and Kirchgässner [5] proved the existence of solitary waves with damped oscillations, bifurcating from a progressive wave with wavenumber  $K$  and with zero amplitude. They reduced the water-wave problem to a system of ordinary differential equations by using the center manifold theorem. They obtained the normal form of this system and showed that it has homoclinic orbits. At least two of these homoclinic orbits persist for the full system. One corresponds to a wave of elevation, the other one to a wave of depression.

In section 2, the water-wave problem is formulated as a dynamical system. In section 3, we propose to construct analytically a good approximation to the wave profile and to the velocity distribution in the flow domain for the waves found by Iooss and Kirchgässner [5], when their amplitude is small. The analysis extends Iooss and Kirchgässner's analysis up to a higher order. In section 4, the limit of both families of waves is taken formally as the water depth becomes infinite. However, the existence proof for the infinite-depth case remains an open problem. Finally, in section 4, a comparison with the numerical results of Hunter and Vanden-Broeck [2], Zufiria [3], and Vanden-Broeck and Dias [6] is made for small-amplitude waves of both elevation and depression.

## 2. Mathematical formulation of the problem

The classical problem of two-dimensional water waves in finite depth when both gravity and surface tension are present is considered. The analysis is made in a frame moving at the velocity  $c$  and only

steady motions in the moving frame are considered. Dimensionless variables are introduced by taking the unit length to be  $T/\rho c^2$  and the unit velocity to be  $c$ . The dimensionless physical coordinates are denoted by  $x$  and  $y$ . The  $x$ -axis is chosen to be the free surface at rest. The  $y$ -axis is directed vertically upwards. The elevation of the free surface above the  $x$ -axis is denoted by  $\eta$ . The bottom lies at  $y = -1/b$ . The velocity components are denoted by  $u$  and  $v$ . The formulation of the problem given below is due to Mielke [14]. Only the choice of unit length is different in ours. The problem is formulated as follows:

$$u_x + v_y = 0, \quad u_y - v_x = 0, \quad \text{for } (x, y) \in \mathbb{R} \times \left(-\frac{1}{b}, \eta\right), \quad (2.1)$$

with the boundary conditions

$$v\left(\cdot, -\frac{1}{b}\right) = 0$$

at the bottom and

$$u\eta_x - v = 0, \quad \frac{1}{2}(u^2 + v^2) + b\lambda\eta - \frac{\eta_{xx}}{(1 + \eta_x^2)^{3/2}} = \frac{1}{2}$$

on the free surface  $y = \eta$ . Equations (2.1) are the continuity and the irrotationality equations. Solitary waves satisfy the asymptotic condition

$$\lim_{x \rightarrow \pm\infty} \begin{pmatrix} u \\ v \end{pmatrix} = \begin{pmatrix} 1 \\ 0 \end{pmatrix}.$$

The streamfunction  $\psi$  is introduced and chosen to be zero on the free surface. It follows that  $\psi$  is equal to  $-1/b$  at the bottom. Next the problem is reformulated by taking  $x$  and  $\psi$  as the independent variables. The velocity components are replaced by the new variables

$$w_1 = \frac{1}{2}(u^2 + v^2 - 1), \quad w_2 = \frac{v}{u}, \quad (2.2)$$

in order to simplify the dynamic boundary condition on the free surface. Physically,  $w_1$  represents the kinetic energy density at the point  $(x, y)$  and  $w_2$  represents the tangent of the angle between the horizontal and the streamline going through  $(x, y)$ . Equations (2.2) can be inverted to give

$$u = \left(\frac{1 + 2w_1}{1 + w_2^2}\right)^{1/2}, \quad v = w_2 \left(\frac{1 + 2w_1}{1 + w_2^2}\right)^{1/2}. \quad (2.3)$$

In terms of the new variables  $w_1$  and  $w_2$ , the formulation (2.1) of the water-wave problem becomes

$$\partial_x \begin{pmatrix} w_1 \\ w_2 \end{pmatrix} = \begin{bmatrix} v & -u^3 \\ u^{-1} & v \end{bmatrix} \partial_\psi \begin{pmatrix} w_1 \\ w_2 \end{pmatrix},$$

where  $u$  and  $v$  are given by (2.3). The boundary conditions become

$$w_2\left(\cdot, -\frac{1}{b}\right) = 0$$

at the bottom, and

$$\eta_x - w_2(\cdot, 0) = 0, \quad w_1(\cdot, 0) + b\lambda\eta - \frac{\eta_{xx}}{(1 + \eta_x^2)^{3/2}} = 0$$

on the free surface. Finally, the trace of  $w_2$  at  $\psi = 0$  is introduced as an extra variable denoted by  $w_0$ . The free-surface elevation  $\eta$  can be expressed in terms of the variables  $w_1$  and  $w_2$ . Dividing the continuity equation by  $u^2$  and integrating with respect to  $\psi$  from  $-1/b$  to 0, one obtains

$$\frac{\partial}{\partial x} \int_{-1/b}^0 \frac{1}{u} d\psi = w_2(\cdot, 0).$$

Since  $w_2(\cdot, 0) = \eta_x$ , it follows that

$$\eta = \int_{-1/b}^0 \frac{1}{u} d\psi - \frac{1}{b}. \quad (2.4)$$

Before starting the analysis, we summarize the formulation of the problem. We wish to solve the equations

$$\begin{aligned} w_{0x} &= (1 + w_0^2)^{3/2} (w_1(\cdot, 0) + \lambda[u^{-1}] - \lambda), & w_{1x} &= v w_{1\psi} - u^3 w_{2\psi}, \\ w_{2x} &= w_{1\psi} u^{-1} + v w_{2\psi}, \end{aligned} \quad (2.5a)$$

where  $[\cdot]$  denotes the mean value of  $\cdot$  over the interval  $[-1/b, 0]$ , together with the boundary conditions

$$w_2(\cdot, 0) = w_0, \quad w_2(\cdot, -b^{-1}) = 0. \quad (2.5b)$$

We observe that the system (2.5a), (2.5b) has a reversibility symmetry. In other words, if the vector  $(w_0(x), w_1(x, \psi), w_2(x, \psi))$  is a solution of the system (2.5a), (2.5b), then the vector  $(-w_0(-x), w_1(-x, \psi), -w_2(-x, \psi))$  is also a solution of the system. Therefore we introduce the matrix  $R$ ,

$$R = \begin{pmatrix} -1 & 0 & 0 \\ 0 & 1 & 0 \\ 0 & 0 & -1 \end{pmatrix}, \quad (2.6)$$

which transforms  $(w_0, w_1, w_2)$  into  $(-w_0, w_1, -w_2)$  and we observe that the right-hand side of (2.5a) anticommutes with  $R$ .

### 3. Analysis

Only the formal aspects of the analysis will be described. The mathematical justification can be found in Iooss et al. [15], Iooss and Kirchgässner [9], and Iooss and Pérouème [16].

Let  $\mathbf{w}$  be the vector of components  $(w_0, w_1, w_2)^T$ . The system (2.5a), (2.5b) to be solved can be written as

$$\partial_x \mathbf{w} = L\mathbf{w} + N(\mathbf{w}), \quad (3.1)$$

where  $L$  is the linearization about  $\mathbf{w} = 0$  and  $N$  a nonlinear operator. The linear operator  $L$  depends on the dimensionless numbers  $b$  and  $\lambda$ , and acts on  $\mathbf{w}$  as follows:

$$L\mathbf{w} = \begin{pmatrix} w_1(\cdot, 0) - \lambda[w_1] \\ -w_{2\psi} \\ w_{1\psi} \end{pmatrix}.$$

The linearization of the equations about the rest state  $\mathbf{w} = 0$  gives

$$\partial_x \mathbf{w} = L\mathbf{w}, \quad (3.2)$$

with the boundary conditions

$$w_2\left(\cdot, -\frac{1}{b}\right) = 0, \quad w_2(\cdot, 0) = w_0.$$

The spectrum of  $L$  is now investigated. It is easy to show that the eigenvalues, denoted by  $\sigma$ , are given by the relation

$$\sigma \cos\left(\frac{\sigma}{b}\right) = (b\lambda - \sigma^2) \sin\left(\frac{\sigma}{b}\right). \quad (3.3)$$

A complete analysis of the spectrum was done by Kirchgässner [17]. When  $\sigma = \pm ib\kappa$ , equation (3.3) becomes the well-known dispersion relation (1.3). It is important to emphasize that so far the analysis has been quite general and applies to the analysis of solitary waves as well as periodic waves.

From now on, the analysis will be restricted to the neighborhood of the curve  $\Gamma$  in the  $(b, \lambda)$ -plane. The curve  $\Gamma$  was described earlier and corresponds to the region where there exists a pair of double imaginary eigenvalues  $\sigma = \pm ib\kappa$ . In the neighborhood above  $\Gamma$ , there exist two solutions  $\mathbf{w}$  of (3.1) which are symmetric with respect to the  $y$ -axis and which tend towards zero as  $x \rightarrow \pm\infty$ . These solutions can be considered as solitary waves, with damped oscillations at infinity of wavenumber  $K$  in addition to the usual single-crest characterizing solitary waves (see fig. 4). One of these solutions has a local maximum at  $x = 0$  for the amplitude of the elevation of the free surface (see plots on the left-hand side of fig. 4) while the other has a local minimum at  $x = 0$  (see plots on the right-hand side of fig. 4). These solutions will be referred to as elevation solitary waves and depression solitary waves. The amplitude of the waves cancels as one approaches the curve  $\Gamma$ , as shown below. Note that  $bh$  is equal to  $T/\rho c^2$ , which is the unit length. Therefore let  $k = b(\kappa)$  be the dimensionless wavenumber, where  $b(\kappa)$  is given by (1.5).

It can be shown that the double eigenvalues  $\pm ik$  are non-semi-simple. The eigenvectors  $\varphi_0^+$ , respectively  $\varphi_0^-$ , and the generalized eigenvectors  $\varphi_1^+$ , respectively  $\varphi_1^-$ , corresponding to the eigenvalue  $+ik$ , respectively  $-ik$ , can be easily calculated. One obtains

$$\varphi_0^+ = \begin{pmatrix} i \tanh \kappa \\ -(\cosh k\psi + \sinh k\psi \tanh \kappa) \\ i(\sinh k\psi + \cosh k\psi \tanh \kappa) \end{pmatrix}, \quad (3.4)$$

$$\varphi_1^+ = \begin{pmatrix} 0 \\ i\psi(\sinh k\psi + \cosh \kappa\psi \tanh \kappa) + (i/b) \cosh k\psi(\tanh \kappa - \coth \kappa) \\ \psi(\cosh k\psi + \sinh k\psi \tanh \kappa) + (1/b) \sinh k\psi(\tanh \kappa - \coth \kappa) \end{pmatrix}, \quad (3.5)$$

and

$$\varphi_0^- = \overline{\varphi_0^+}, \quad \varphi_1^- = \overline{\varphi_1^+}.$$

It should be emphasized that the vectors  $\varphi_0^+$  and  $\varphi_1^+$  are not unique. Any multiple of  $\varphi_0^+$  is also an eigenvector and any vector of the form  $\varphi_1^+ + \gamma\varphi_0^+$  is also a generalized eigenvector. Our particular choice for  $\varphi_0^+$  and  $\varphi_1^+$  was made in such a way that the limiting process as  $\kappa$  approaches infinity provides “nice” limits for all the coefficients computed below. We observe that  $R\varphi_0^+ = \varphi_0^-$  and that  $R\varphi_1^+ = -\varphi_1^-$ .

Since we look for solutions with  $(b, \lambda)$  close to the curve  $\Gamma$ , we define a small parameter  $m = b^*(\lambda - \lambda^*)$ , where the stars refer to values on the curve  $\Gamma$ . For a bifurcating solution to exist, the parameter  $m$  must be positive. The center manifold reduction theorem can be used here, as shown in Iooss and Kirchgässner [9]. This means that all solutions of (3.1), staying small and bounded for  $x \in (-\infty, +\infty)$ , can be written in the form

$$\mathbf{w} = A\varphi_0^+ + B\varphi_1^+ + \bar{A}\varphi_0^- + \bar{B}\varphi_1^- + \Phi(m; A, B, \bar{A}, \bar{B}), \quad (3.6)$$

where  $\Phi$  consists of higher-order terms in  $A, B, \bar{A}, \bar{B}$ . We now have to study the reduced ordinary differential equations in the amplitudes  $A$  and  $B$

$$\begin{cases} A_x = ikA + B + f(m; A, B, \bar{A}, \bar{B}), \\ B_x = ikB + g(m; A, B, \bar{A}, \bar{B}), \end{cases} \quad (3.7)$$

where  $f$  and  $g$  are terms of higher order. The next (and essential) step consists of finding  $A$  and  $B$  to a given order. Once  $A$  and  $B$  are known, one has an expression for  $\mathbf{w}$  given by (3.6), i.e. an expression for  $w_1$  and  $w_2$ . Then  $u$  and  $v$  can be obtained from (2.3). Finally, the free-surface elevation  $\eta$  can be calculated from (2.4).

A powerful method for finding  $A$  and  $B$  consists of using normal form theory. The idea behind using normal form theory is to make the right choice of coordinates which gives the most simple form to (3.7). For instance, the normal form for the Hopf bifurcation consists in adapting the coordinates in such a way that the bifurcating closed orbit becomes a circle, hence easy to see on the new system. Our case is more complicated, because it combines the 1:1 resonance normal form (double non-semi-simple eigenvalues  $\pm ik$ ) with reversibility. As shown in detail for instance in Iooss and Adelmeyer [18], the system (3.7) can be put in the form

$$\begin{aligned} A_x &= ikA + B + iAP(m; |A|^2, \tfrac{1}{2}i(A\bar{B} - \bar{A}B)), \\ B_x &= ikB + iBP(m; |A|^2, \tfrac{1}{2}i(A\bar{B} - \bar{A}B)) + AQ(m; |A|^2, \tfrac{1}{2}i(A\bar{B} - \bar{A}B)). \end{aligned} \quad (3.8)$$



The new coordinates are still denoted by  $A$  and  $B$ , if we notice that the change of variable has the effect of suitably choosing the function  $\Phi$  in (3.6). Choosing the good representation for  $\Phi$  gives the polynomials  $P$  and  $Q$  with real coefficients in their arguments. We write them as

$$\begin{aligned} P(m; |A|^2, \tfrac{1}{2}i(\bar{A}\bar{B} - \bar{A}B)) &= p_1 m + p_2 |A|^2 + \tfrac{1}{2} p_3 i(\bar{A}\bar{B} - \bar{A}B) + \cdots, \\ Q(m; |A|^2, \tfrac{1}{2}i(\bar{A}\bar{B} - \bar{A}B)) &= q_1 m - q_2 |A|^2 + \tfrac{1}{2} q_3 i(\bar{A}\bar{B} - \bar{A}B) + \cdots. \end{aligned} \quad (3.9)$$

The equations (3.8) combined with (3.9) are valid up to an arbitrary fixed order  $(|A| + |B|)^N$ .

The next step consists of computing the four coefficients  $p_1, p_2, q_1, q_2$ . The coefficients  $p_1$  and  $q_1$  are easy to obtain if one observes that they are related to the eigenvalues of the linearization of (3.8) about  $(0, 0)$ . The eigenvalues are

$$\sigma = i[k + P(m; 0, 0)] \pm \sqrt{Q(m; 0, 0)},$$

or

$$\sigma = i[k + p_1 m] \pm \sqrt{q_1} \sqrt{m} + \mathcal{O}(m^{3/2}). \quad (3.10)$$

If we substitute this expression into (3.3) with  $b\lambda = b^* \lambda^* + m$  and expand in powers of  $m$ , one finds that

$$q_1(\kappa) = \frac{\sinh \kappa \cosh \kappa - \kappa}{\sinh \kappa \cosh \kappa + \kappa - 2\kappa^2 \coth \kappa} \quad (3.11)$$

and

$$p_1(\kappa) = \frac{2\kappa^2(-3\sinh \kappa \cosh \kappa + 2\kappa \cosh^2 \kappa + \kappa)}{3(\sinh \kappa \cosh \kappa + \kappa - 2\kappa^2 \coth \kappa)^2}. \quad (3.12)$$

It can be shown that both coefficients  $p_1$  and  $q_1$  are positive functions of  $\kappa$ , which decrease monotonically as  $\kappa$  increases. The asymptotic behaviors of  $p_1$  and  $q_1$  are

$$p_1 \sim \frac{16}{3} \kappa^3 \exp(-2\kappa), \quad q_1 \sim 1 + 8\kappa^2 \exp(-2\kappa), \quad \text{for } \kappa \rightarrow \infty,$$

and

$$p_1 \sim \frac{45}{8} \kappa^{-3}, \quad q_1 \sim \frac{15}{4} \kappa^{-2}, \quad \text{for } \kappa \rightarrow 0.$$

The coefficients  $p_2$  and  $q_2$  are more difficult to compute. Let us set  $m=0$  in the following computations since this does not change anything. We follow the method developed in Iooss et al. [15] (see their appendix 3). Equation (3.1) can be rewritten as

$$\mathbf{w}_x = L\mathbf{w} + N_2(\mathbf{w}, \mathbf{w}) + N_3(\mathbf{w}, \mathbf{w}, \mathbf{w}) + \cdots, \quad (3.13)$$

where  $N_2$  denotes the quadratic terms in the components  $w_1$  and  $w_2$  of the nonlinear operator  $N$

$$N_2(\mathbf{w}, \mathbf{w}) = \begin{cases} \frac{1}{2} \lambda^*(3[w_1^2] + [w_2^2]), \\ w_2 w_{1\psi} - 3w_1 w_{2\psi}, \\ -w_1 w_{1\psi} + w_2 w_{2\psi}, \end{cases} \quad (3.14)$$

and  $N_3$  denotes the cubic terms

$$N_3(\mathbf{w}, \mathbf{w}, \mathbf{w}) = \begin{cases} \frac{3}{2} w_0^2(w_1(\cdot, 0) - \lambda^*[w_1]) - \frac{1}{2} \lambda^*(5[w_1^3] + [w_1 w_2^2]), \\ w_1 w_2 w_{1\psi} - \frac{3}{2} w_{2\psi}(w_1^2 - w_2^2), \\ \frac{1}{2}(3w_1^2 + w_2^2)w_{1\psi} + w_2 w_1 w_{2\psi}. \end{cases} \quad (3.15)$$

The dots denote higher-order terms. Another expression for  $\mathbf{w}_x$  can be obtained by differentiating (3.6) with respect to  $x$  and setting  $m = 0$ :

$$\mathbf{w}_x = A_x \varphi_0^+ + B_x \varphi_1^+ + \bar{A}_x \varphi_0^- + \bar{B}_x \varphi_1^- + \Phi_x(0; A, B, \bar{A}, \bar{B}). \quad (3.16)$$

Next we give the first terms in the expansion of  $\Phi$ :

$$\begin{aligned} \Phi(0; A, B, \bar{A}, \bar{B}) = & (A^2 \Phi_{2000} + \text{c.c.}) + |A|^2 \Phi_{1100} + (AB \Phi_{1010} + \text{c.c.}) + (\bar{A} \bar{B} \Phi_{0110} + \text{c.c.}) \\ & + (A^3 \Phi_{3000} + \text{c.c.}) + (A|A|^2 \Phi_{2100} + \text{c.c.}) + (A^4 \Phi_{4000} + \text{c.c.}) + |A|^4 \Phi_{2200} \\ & + (A^3 \bar{A} \Phi_{3100} + \text{c.c.}) + (A^2 \bar{B} \Phi_{2010} + \text{c.c.}) + (|A|^2 \bar{B} \Phi_{1110} + \text{c.c.}) \\ & + (A^2 \bar{B} \Phi_{2001} + \text{c.c.}) + (B^2 \Phi_{0020} + \text{c.c.}) + |B|^2 \Phi_{0011} + \dots, \end{aligned}$$

where c.c. stands for complex conjugate. If  $A_x$  and  $B_x$  are replaced in (3.16) by their expressions from (3.8), we can equate the powers of  $A$ ,  $B$  and so on in (3.13) and (3.16). It leads to the following system of equations:

$$L\varphi_0^+ = ik\varphi_0^+, \quad (3.17)$$

$$L\varphi_1^+ = ik\varphi_1^+ + \varphi_0^+, \quad (3.18)$$

$$L\Phi_{2000} + N_2(\varphi_0^+, \varphi_0^+) = 2ik\Phi_{2000}, \quad (3.19)$$

$$L\Phi_{1100} + 2N_2(\varphi_0^+, \varphi_0^-) = 0, \quad (3.20)$$

$$\begin{aligned} L\Phi_{2100} + 2N_2(\varphi_0^+, \Phi_{1100}) + 2N_2(\varphi_0^-, \Phi_{2000}) \\ + 3N_3(\varphi_0^+, \varphi_0^+, \varphi_0^-) = ik\Phi_{2100} + ip_2\varphi_0^+ - q_2\varphi_1^+, \end{aligned} \quad (3.21)$$

$$\begin{aligned} L\Phi_{1110} + 2N_2(\varphi_1^+, \Phi_{1100}) + 2N_2(\varphi_0^-, \Phi_{1010}) \\ + 2N_2(\varphi_0^+, \Phi_{0110}) + 6N_3(\varphi_0^+, \varphi_0^-, \varphi_1^+) = ik\Phi_{1110} + \frac{1}{2}p_3\varphi_0^+ + i(p_2 - \frac{1}{2}q_3)\varphi_1^+ + 2\Phi_{2100}, \end{aligned} \quad (3.22)$$

$$L\Phi_{2001} + 2N_2(\varphi_1^-, \Phi_{2000}) + 2N_2(\varphi_0^+, \Phi_{1001}) + 3N_3(\varphi_0^+, \varphi_0^+, \varphi_1^-) = ik\Phi_{2001} - \frac{1}{2}p_3\varphi_0^+ + \frac{1}{2}iq_3\varphi_1^+ + \Phi_{2100}, \quad (3.23)$$

$$L\Phi_{1010} + 2N_2(\varphi_0^+, \varphi_1^+) = 2ik\Phi_{1010} + 2\Phi_{2000}, \quad (3.24)$$

$$L\Phi_{0110} + 2N_2(\varphi_0^-, \varphi_1^+) = \Phi_{1100}. \quad (3.25)$$

In order to calculate the coefficients  $p_2$  and  $q_2$ , one has to introduce the adjoint operator  $L^*$  of  $L$  which is such that

$$\langle L\mathbf{w}, \mathbf{v} \rangle = \langle \mathbf{w}, L^*\mathbf{v} \rangle, \quad \mathbf{w} \in D(L), \quad \mathbf{v} = (v_0, v_1, v_2)^T \in D(L^*),$$

where the scalar product  $\langle \mathbf{w}, \mathbf{v} \rangle$  is defined as

$$\langle \mathbf{w}, \mathbf{v} \rangle = w_0 \overline{v_0} + \int_{-1/b}^0 w_1 \overline{v_1} d\psi + \int_{-1/b}^0 w_2 \overline{v_2} d\psi. \quad (3.26)$$

The domains  $D(L)$  and  $D(L^*)$  are such that they contain the boundary conditions

$$\left\{ w_2\left(\cdot, -\frac{1}{b}\right) = 0, w_2(\cdot, 0) = w_0 \right\} \quad \text{for } D(L),$$

and

$$\left\{ v_2\left(\cdot, -\frac{1}{b}\right) = 0, v_2(\cdot, 0) = -v_0 \right\} \quad \text{for } D(L^*).$$

The operator  $L^*$  is defined as follows:

$$L^*\mathbf{v} = \begin{pmatrix} -v_1(\cdot, 0) \\ -v_{2\psi} + b\lambda v_2(\cdot, 0) \\ v_{1\psi} \end{pmatrix}.$$

The eigenvectors  $\psi_+^1$  and generalized eigenvectors  $\psi_+^0$  for the adjoint operator  $L^*$  satisfy

$$L^*\psi_+^1 = -ik\psi_+^1, \quad L^*\psi_+^0 = -ik\psi_+^0 + \psi_+^1,$$

and can be chosen so that

$$\langle \varphi_0^+, \psi_+^1 \rangle = 0, \quad \langle \varphi_0^+, \psi_+^0 \rangle = 1, \quad \langle \varphi_1^+, \psi_+^1 \rangle = 1, \quad \langle \varphi_1^+, \psi_+^0 \rangle = 0.$$

One finds that

$$\psi_+^1 = \mathcal{P}_0 \begin{pmatrix} 1 \\ i(\cosh k\psi \coth \kappa + \sinh k\psi) - i\frac{\lambda^*}{\kappa} \\ -(\sinh k\psi \coth \kappa + \cosh k\psi) \end{pmatrix} \quad (3.27)$$

and

$$\psi_+^0 = \mathcal{P}_0 \begin{pmatrix} 0 \\ -\psi(\sinh k\psi \coth \kappa + \cosh k\psi) + \frac{\cosh k\psi}{b \sinh^2 \kappa} - \frac{b\lambda^*}{k^2} \\ -i\psi(\cosh k\psi \coth \kappa + \sinh k\psi) + i \frac{\sinh k\psi}{b \sinh^2 \kappa} \end{pmatrix} + i\mathcal{P}_1 \psi_+^1. \quad (3.28)$$

The constant  $\mathcal{P}_0$  is equal to

$$\mathcal{P}_0(\kappa) = \frac{\cosh \kappa (\sinh \kappa \cosh \kappa - \kappa)^2}{2 \sinh^2 \kappa (\sinh^2 \kappa \cosh \kappa + \kappa \sinh \kappa - 2\kappa^2 \cosh \kappa)},$$

with

$$\mathcal{P}_0 \sim \frac{1}{2} \quad \text{as } \kappa \rightarrow \infty \quad \text{and} \quad \mathcal{P}_0 \sim \frac{5}{4} \kappa^{-2} \quad \text{as } \kappa \rightarrow 0.$$

The constant  $\mathcal{P}_1$  is equal to

$$\mathcal{P}_1(\kappa) = \frac{6 \sinh^3 \kappa \cosh \kappa + 6\kappa \sinh^2 \kappa - 4(2 \cosh^2 \kappa + 1)\kappa^3}{3(\sinh \kappa \cosh \kappa - \kappa)(\sinh \kappa \cosh \kappa + \kappa - 2\kappa^2 \coth \kappa)},$$

with

$$\mathcal{P}_1 \sim 2 \quad \text{as } \kappa \rightarrow \infty \quad \text{and} \quad \mathcal{P}_1 \sim \frac{4}{7} \kappa \quad \text{as } \kappa \rightarrow 0.$$

Both  $\mathcal{P}_0$  and  $\mathcal{P}_1$  are positive for all  $\kappa$ . We observe that  $R\psi_+^1 = -\psi_-^1$  and  $R\psi_+^0 = \psi_-^0$ .

With this choice of eigenvectors and generalized eigenvectors, the projection  $\Pi$  of  $\mathbf{w}$  on the invariant subspace spanned by  $\varphi_0^+$ ,  $\varphi_0^-$ ,  $\varphi_1^+$ ,  $\varphi_1^-$ , which commutes with  $L$  for  $b\lambda = b^*\lambda^*$ , is as follows:

$$\Pi \mathbf{w} = \langle \mathbf{w}, \psi_+^0 \rangle \varphi_0^+ + \langle \mathbf{w}, \psi_+^1 \rangle \varphi_1^+ + \langle \mathbf{w}, \psi_-^0 \rangle \varphi_0^- + \langle \mathbf{w}, \psi_-^1 \rangle \varphi_1^-.$$

By adding (3.22) and (3.23) and taking the scalar product with  $\psi_+^1$ , one obtains

$$\begin{aligned} ip_2 = & -3\langle \Phi_{2100}, \psi_+^1 \rangle + \langle 2N_2(\varphi_1^+, \Phi_{1100}) + 2N_2(\varphi_0^-, \Phi_{1010}) \\ & + 2N_2(\varphi_0^+, \Phi_{0110}) + 6N_3(\varphi_0^+, \varphi_0^-, \varphi_1^+) + 2N_2(\varphi_1^-, \Phi_{2000}) \\ & + 2N_2(\varphi_0^+, \Phi_{1001}) + 3N_3(\varphi_0^+, \varphi_0^+, \varphi_1^-), \varphi_+^1 \rangle. \end{aligned} \quad (3.29)$$

By taking the scalar product of (3.21) with  $\psi_0^+$ , one obtains

$$\langle \Phi_{2100}, \psi_+^1 \rangle = ip_2 - \langle 2N_2(\varphi_0^+, \Phi_{1100}) + 2N_2(\varphi_0^-, \Phi_{2000}) + 3N_3(\varphi_0^+, \varphi_0^+, \varphi_0^-), \psi_+^0 \rangle. \quad (3.30)$$

Therefore, combining (3.29) and (3.30) yields

$$\begin{aligned} 4ip_2 = & \langle 2N_2(\varphi_1^+, \Phi_{1100}) + 2N_2(\varphi_0^-, \Phi_{1010}) + 2N_2(\varphi_0^+, \Phi_{0110}) + 6N_3(\varphi_0^+, \varphi_0^-, \varphi_1^+) \\ & + 2N_2(\varphi_1^-, \Phi_{2000}) + 2N_2(\varphi_0^+, \Phi_{1001}) + 3N_3(\varphi_0^+, \varphi_0^+, \varphi_1^-), \psi_+^1 \rangle \\ & + 3\langle 2N_2(\varphi_0^+, \Phi_{1100}) + 2N_2(\varphi_0^-, \Phi_{2000}) + 3N_3(\varphi_0^+, \varphi_0^+, \varphi_0^-), \psi_+^0 \rangle. \end{aligned} \quad (3.31)$$

The coefficient  $q_2$  is obtained by taking the scalar product of (3.21) with  $\psi_+^1$ :

$$q_2 = -\langle 2N_2(\varphi_0^+, \Phi_{1100}) + 2N_2(\varphi_0^-, \Phi_{2000}) + 3N_3(\varphi_0^+, \varphi_0^+, \varphi_0^-), \psi_+^1 \rangle. \quad (3.32)$$

All the computations needed to find  $p_2$  and  $q_2$  can be easily performed symbolically. The symbolic package “MAPLE” was used by the authors. The vectors  $\Phi_{2000}$ ,  $\Phi_{1100}$ ,  $\Phi_{1010}$ ,  $\Phi_{0110}$ , as well as the full expressions for  $p_2(\kappa)$  and  $q_2(\kappa)$ , are given in the appendix. Here, we just give the asymptotic values of  $p_2$  and  $q_2$  for  $\kappa$  large and small:

$$p_2 \sim \frac{5}{8} + \frac{4}{\kappa}, \quad q_2 \sim \frac{11}{8} + \frac{2}{\kappa}, \quad \text{for } \kappa \text{ large},$$

and

$$p_2 \sim -\frac{16425}{32} \kappa^{-7}, \quad q_2 \sim \frac{4275}{8} \kappa^{-6}, \quad \text{for } \kappa \text{ small}.$$

The coefficient  $q_2$  is a positive function of  $\kappa$ , which decreases monotonically from infinity to  $11/8$  as  $\kappa$  increases from zero to infinity. Since the coefficient  $p_2$  appears only in the ratio  $p_2/q_2$  below, a plot of  $p_2/q_2$  versus  $\kappa$  is given in fig. 3. The ratio  $p_2/q_2$  has a maximum 0.9692 for  $\kappa = 3.8588$  and vanishes for  $\kappa = 1.3100$ .

The next step is to integrate (3.8) with respect to  $x$ . We write

$$A(x) = r_0(x) e^{i(kx + \theta_0)}, \quad B(x) = r_1(x) e^{i(kx + \theta_1)}.$$

It is observed in Iooss et al. [15] that the system (3.8) is integrable, one of the first integrals being  $A\bar{B} - \bar{A}B = \mathcal{C}$ . It is also observed in Iooss and P  rou  me [16] that for  $q_2 > 0$ , the case  $\mathcal{C} = 0$  gives homoclinic orbits. Indeed let

$$A\bar{B} - \bar{A}B = 2ir_0r_1 \sin(\theta_0 - \theta_1) = 0.$$

Therefore  $\theta_0 - \theta_1 = 0$  or  $\theta_0 - \theta_1 = \pi$ . We can assume  $\theta_0 - \theta_1 = 0$  and allow  $r_1$  to take negative values, so that, after replacing  $A$  and  $B$  by their expression in (3.8), we obtain the following system:

$$\frac{dr_0}{dx} = r_1, \quad (3.33)$$

$$\frac{dr_1}{dx} = r_0 Q(m; r_0^2, 0), \quad (3.34)$$

$$\frac{d\theta_0}{dx} = P(m; r_0^2, 0). \quad (3.35)$$

Equations (3.33) and (3.34) can be combined to give

$$\frac{d^2 r_0}{dx^2} = r_0 Q(m; r_0^2, 0) = mq_1 r_0 - q_2 r_0^3 + \cdots,$$

which can be integrated to give

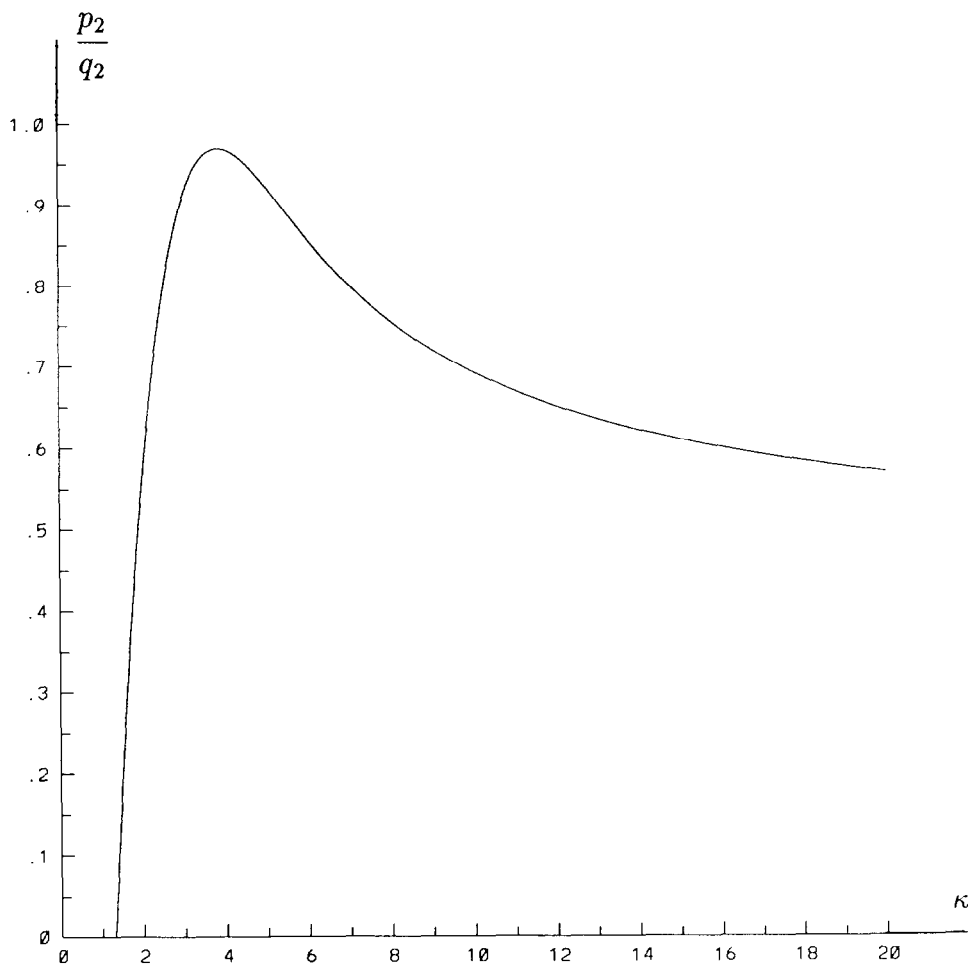


Fig. 3. Plot of the ratio  $p_2/q_2$  versus  $\kappa$ . Negative values of  $p_2/q_2$  are not shown.

$$\left(\frac{dr_0}{dx}\right)^2 = \int_0^{r_0^2} Q(m; r, 0) dr = r_0^2(mq_1 - \frac{1}{2}q_2r_0^2) + \dots + \text{constant}. \quad (3.36)$$

The constant is taken to be zero in order to obtain the homoclinic orbits which lead to the solitary waves. Let us introduce the rescaling

$$q_2r_0^2 = 2mq_1\rho_0^2, \quad q_2\left(\frac{dr_0}{dx}\right)^2 = 2m^2q_1^2\left(\frac{d\rho_0}{d\xi}\right)^2,$$

where  $\xi = \sqrt{mq_1}x$ .

Equation (3.36) reduces to

$$\left(\frac{d\rho_0}{d\xi}\right)^2 = \rho_0^2 - \rho_0^4 + \dots, \quad (3.37)$$

where the dots denote terms of order  $m$  and above. Neglecting the higher-order terms, (3.37) can be explicitly integrated to give for the even solutions (which lead to the reversible orbits)

$$\rho_0 = \pm \frac{1}{\cosh \xi}.$$

It follows that

$$r_0(x) = \pm \sqrt{\frac{2mq_1}{q_2}} \frac{1}{\cosh(\sqrt{mq_1}x)}, \quad (3.38)$$

$$r_1(x) = \mp mq_1 \sqrt{\frac{2}{q_2}} \frac{\sinh(\sqrt{mq_1}x)}{\cosh(\sqrt{mq_1}x)^2}. \quad (3.39)$$

There is in fact a one-parameter family of homoclinic solutions of the truncated system, but Iooss and Pérouème [16] showed that the homoclinic solutions which are reversible persist for the full system. There are two such reversible solutions, corresponding to the plus and minus signs in (3.38). The expressions (3.38) for  $r_0$  are exact up to order  $m$ . The higher-order terms are of order  $m\sqrt{m}$  and above. It is important to emphasize that, since  $q_1$  and  $q_2$  depend only on  $\kappa$ ,  $r_0(x)$  and  $r_1(x)$  depend on the two parameters  $m$  and  $\kappa$ , or, in terms of physical parameters, on  $b$  and  $\lambda$ .

Equation (3.35), which is

$$\frac{d\theta_0}{dx} = p_1 m + p_2 r_0^2 + \dots,$$

can be integrated to give

$$\theta_0(x) = p_1 mx + 2 \frac{p_2}{q_2} \sqrt{mq_1} \tanh(\sqrt{mq_1}x) + \dots. \quad (3.40)$$

Having computed  $A$  and  $B$ , we obtain from (3.6) an expression for  $w$  exact up to order  $m$ . It follows that we also have an expression for the velocity vector  $(u, v)$  in the whole flow field, which is obtained from (2.3). The elevation of the free surface can be easily obtained from (2.4). There are two types of waves: elevation solitary waves ( $\eta(0) > 0$ ) and depression solitary waves ( $\eta(0) < 0$ ). Their profile is given by

$$\eta = \frac{1}{b} (-[w_1] + \tfrac{1}{2}[3w_1^2 + w_2^2] + \dots).$$

To second order in  $\sqrt{m}$ , the elevation of the free surface for the elevation wave and for the depression wave is

$$\begin{aligned} \eta(x) = & 2r_0(x) \cos kx \frac{\tanh \kappa}{k} + 2r_1(x) \sin kx \frac{\tanh \kappa}{k^2} \left( \frac{2kp_2}{q_2} - 1 \right) \\ & + r_0^2(x) \cos 2kx (1 - \mathcal{A}) \frac{\tanh \kappa}{k} - r_0^2(x) \frac{\kappa + \sinh 2\kappa}{k(\lambda^* - 1) \cosh^2 \kappa}, \end{aligned} \quad (3.41)$$

where  $r_0(x)$  is given by (3.38) with the plus sign for the elevation wave (minus sign for the depression

wave),  $r_1(x) = r'_0(x)$ ,  $k = b\kappa$  and  $p_2(\kappa)$ ,  $q_2(\kappa)$ ,  $\mathcal{A}(\kappa)$  can be found in the appendix. The function  $\mathcal{A}(\kappa)$  comes from the vector  $\Phi_{2000}$ .

We have now completed the analytical construction of an approximation to the solitary waves found by Iooss and Kirchgässner [5]. The last equation (3.41) provides the profile of the waves. The waves depend on the parameters  $\kappa$  and  $m$ , or, in terms of physical parameters, on the dimensionless numbers  $b$  and  $\lambda$ . The approximation is not valid as  $\kappa \rightarrow 0$  (because the structure of the spectrum changes) and as  $m$  becomes large (because terms of higher order have been neglected). In other words, (3.41) can be used to compute solitary waves for values of  $(b, \lambda)$  slightly above the curve  $\Gamma$  shown in fig. 1 and not too close to the point  $(\frac{1}{3}, 1)$ . In section 5, eq. (3.41) will be plotted for different values of  $m$  and  $\kappa$ . The effects of the parameters  $\kappa$  and  $m$  will be studied. It will be shown that, if  $\kappa$  is fixed and  $m$  is decreased towards zero, the waves become “more and more periodic” and the amplitude of oscillations approaches zero. In the limit  $m = 0$ , periodic waves of “zero” amplitude with wavenumber  $k$  are obtained. As  $m$  becomes larger, the waves decay faster towards infinity.

#### 4. Infinite depth

The case of infinite depth is interesting because it provides solitary waves in infinite depth. Such depression waves were first computed by Longuet-Higgins [4]. Vanden-Broeck and Dias [6] computed both elevation and depression waves from small amplitude up to the limiting configurations with trapped bubbles. Below, the limit of the results of the previous section as  $h$  approaches infinity will be taken. We emphasize here that the limiting process is purely formal. A rigorous proof that the limit can be taken is currently being constructed. As  $h \rightarrow \infty$ , the formulation of the problem (2.5a), (2.5b) becomes

$$w_{0x} = (1 + w_0^2)^{3/2} \left[ w_1(\cdot, 0) + \lim_{b \rightarrow 0} b\lambda \int_{-1/b}^0 \left( \frac{1}{u} - 1 \right) d\psi \right],$$

$$w_{1x} = uw_{1\psi} - u^3 w_{2\psi},$$

$$w_{2x} = \frac{w_{1\psi}}{u} + uw_{2\psi},$$

with the boundary conditions

$$w_2(\cdot, 0) = w_0, \quad w_2(\cdot, -\infty) = 0.$$

As  $\kappa \rightarrow \infty$ ,

$$b \sim \frac{1}{2\kappa}, \quad \lambda \sim \frac{1}{2}\kappa, \quad b\lambda \sim \frac{1}{4}.$$

The dispersion relation (1.3) takes the simple form

$$\left( \frac{1}{4} + k^2 \right) - k = 0$$



and the eigenvalues  $\pm ik$  of the linear operator  $L$  become  $\pm \frac{1}{2}i$ . The perturbed eigenvalues given by (3.10) become

$$\sigma = \frac{1}{2}i \pm \sqrt{m}.$$

The eigenvectors (3.4) and (3.5) and the generalized eigenvectors (3.27) and (3.28) become

$$\begin{aligned} \varphi_0^+ &= \begin{pmatrix} i \\ -\exp \frac{1}{2}\psi \\ i \exp \frac{1}{2}\psi \end{pmatrix}, & \varphi_1^+ &= \begin{pmatrix} 0 \\ i\psi \exp \frac{1}{2}\psi \\ \psi \exp \frac{1}{2}\psi \end{pmatrix}, \\ \psi_+^1 &= \begin{pmatrix} \frac{1}{2} \\ \frac{1}{2}i \exp \frac{1}{2}\psi - \frac{1}{4}i \\ -\frac{1}{2} \exp \frac{1}{2}\psi \end{pmatrix}, & \psi_+^0 &= \begin{pmatrix} i \\ -\frac{1}{2}\psi \exp \frac{1}{2}\psi - \exp \frac{1}{2}\psi \\ -\frac{1}{2}i\psi \exp \frac{1}{2}\psi - i \exp \frac{1}{2}\psi \end{pmatrix}. \end{aligned}$$

The vectors  $\Phi_{2000}$  (see (A.1)) and  $\Phi_{1010}$  (see (A.4)) become

$$\Phi_{2000} = \begin{pmatrix} -4i \\ 5 \exp \psi \\ -4i \exp \psi \end{pmatrix}, \quad \text{and} \quad \Phi_{1010} = \begin{pmatrix} 24 \\ 24i \exp \psi - 10i\psi \exp \psi \\ 24 \exp \psi - 8\psi \exp \psi \end{pmatrix}.$$

The amplitude and phase (3.38)–(3.40) become

$$r_0 = \pm 4\sqrt{\frac{m}{11}} \frac{1}{\cosh \sqrt{m}x}, \quad r_1 = \frac{dr_0}{dx}, \quad \theta_0 = \frac{10\sqrt{m}}{11} \tanh \sqrt{m}x.$$

The elevations of the free surface (to second order in  $\sqrt{m}$ ) for the elevation wave and for the depression wave become

$$\eta(x) = \pm \frac{16\sqrt{m}}{\sqrt{11}} \frac{\cos \frac{1}{2}x}{\cosh \sqrt{m}x} \pm \frac{192m}{11\sqrt{11}} \frac{\sinh \sqrt{m}x \sin \frac{1}{2}x}{\cosh^2 \sqrt{m}x} - \frac{128m}{11} \frac{\cos x}{\cosh^2 \sqrt{m}x}.$$

## 5. Results and comparison with numerical results

In this section, solitary-wave profiles based on the analytical construction of section 3 are plotted for different values of  $\kappa$  and  $m$ . Roughly speaking, the parameter  $\kappa$  measures the water depth. The parameter  $m$  measures the distance from the bifurcation curve and is closely related to the maximum amplitude of the waves. Comparisons are made with numerical results of Hunter and Vanden-Broeck [2], Zufiria [3], and Vanden-Broeck and Dias [6].

The results based on the analytical method developed in section 3 are valid only for small amplitude waves and for  $\kappa$  not too close to zero. In fig. 4, solitary waves of elevation and depression have been plotted for  $\kappa = 2$ , which might be considered as an *intermediate* value for  $\kappa$ . The corresponding values for the dimensionless numbers  $b$  and  $\lambda$  on the curve  $\Gamma$  defined in the introduction by (1.5), (1.6) are

$$b = 0.2213 \quad \text{and} \quad \lambda = 1.1894.$$

The Froude number is 0.9169. As  $m$  increases, the oscillations decay more rapidly and the maximum

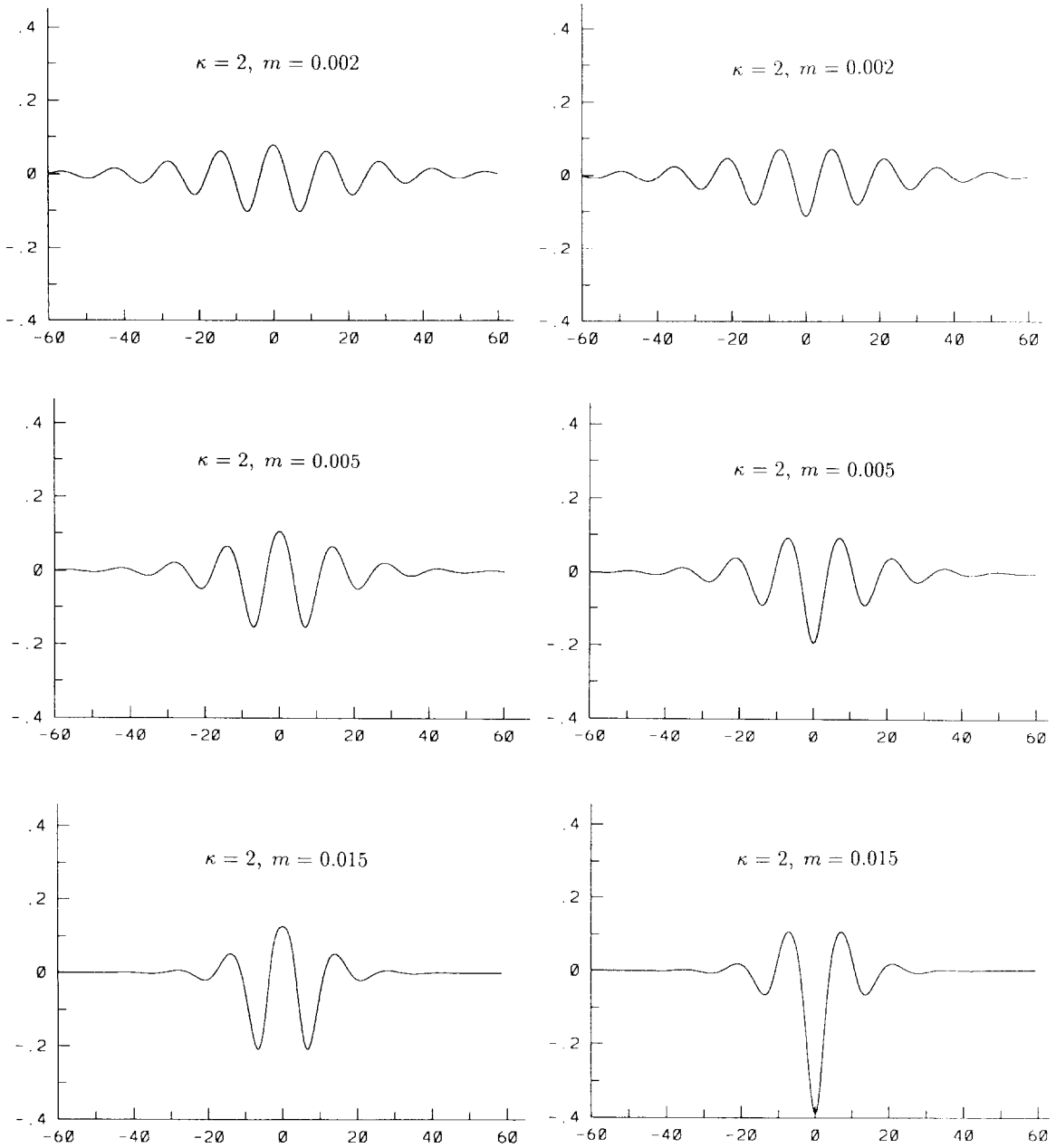


Fig. 4. Solitary-wave profiles for  $\kappa = 2$  based on analytical results: (left) elevation waves, (right) depression waves.

amplitude of the wave, defined as  $|\eta(0)|$ , increases. The increase is more rapid for the depression wave. The wavelength of the oscillations is approximately equal to  $2\pi/b\kappa = 14.20$  (recall that the unit length is  $T/\rho c^2$ ). If  $\rho$  and  $T$  are replaced by their values for water, one finds the following values for the physical parameters:

$$h = 0.64 \text{ cm}, \quad c = 22.9 \text{ cm/s}, \quad l = 2 \text{ cm},$$

where  $l$  is the wavelength of the oscillations. When  $\kappa$  varies on the bifurcation curve from zero to infinity, the wave velocity varies from  $c = 21.6$  cm/s to  $c = 23.2$  cm/s, and the water depth varies from  $h = 0.48$  cm to infinity.

Figure 4 shows how the shape of the waves varies with  $m$  for  $\kappa$  fixed. On the other hand, fig. 5 shows how the amplitude at the origin varies with  $\kappa$  for  $m = 0.01$ . One sees that  $|\eta(0)|$  decreases as  $\kappa$  decreases.

In section 4, the formal limit of the problem as the water depth becomes large was taken. The approximate wavelength of the oscillations is  $4\pi$  or 12.57. The physical values for water are  $c = 23.2$  cm/s and  $l = 1.73$  cm. Figure 6 shows the profiles of the deep-water elevation and depression waves corresponding to  $m = 0.005$ . They are compared with the profiles obtained by the numerical scheme used by Vanden-Broeck and Dias [6], which is based on the solution of an integro-differential equation. The agreement is good. It is, however, better for the elevation wave than for the depression wave, for which the numerical decay of the oscillations seems to be faster than the analytical decay. But for some other water depths, the agreement was found to be better for the depression wave than for the elevation wave.

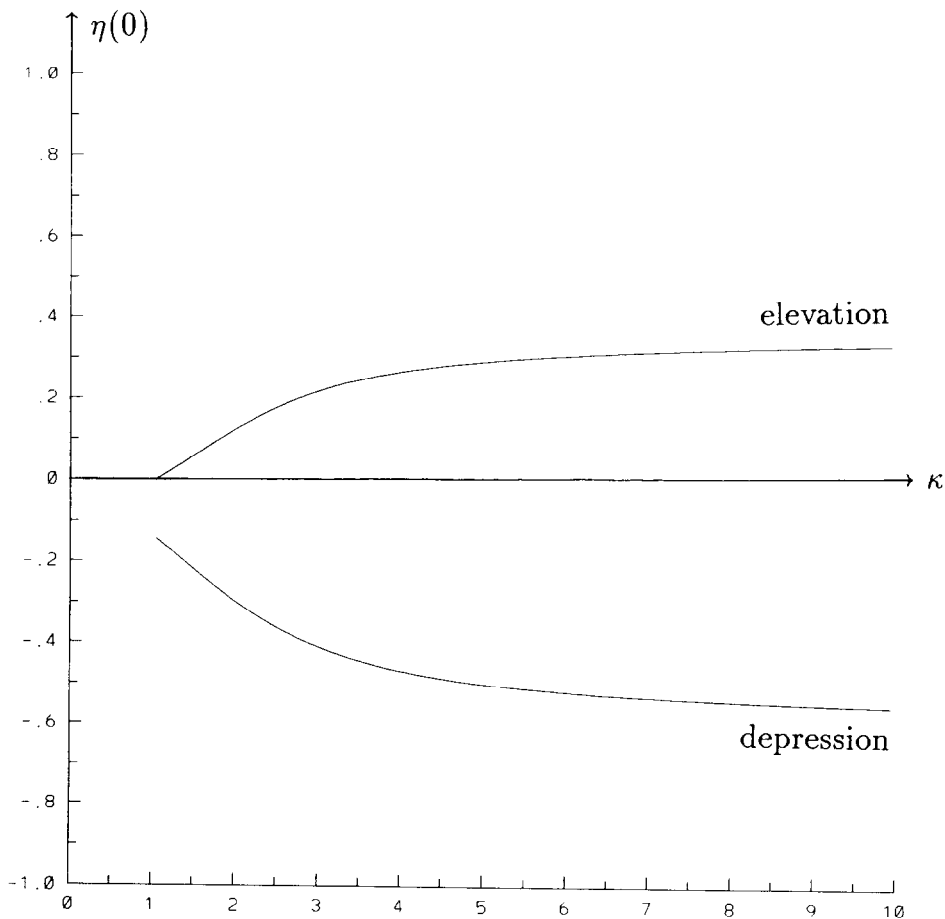


Fig. 5. Plot of  $\eta(0)$  versus  $\kappa$  for  $m = 0.01$ . The analysis is not valid for small values of  $\kappa$ .

$$\kappa \rightarrow \infty, m = 0.005$$

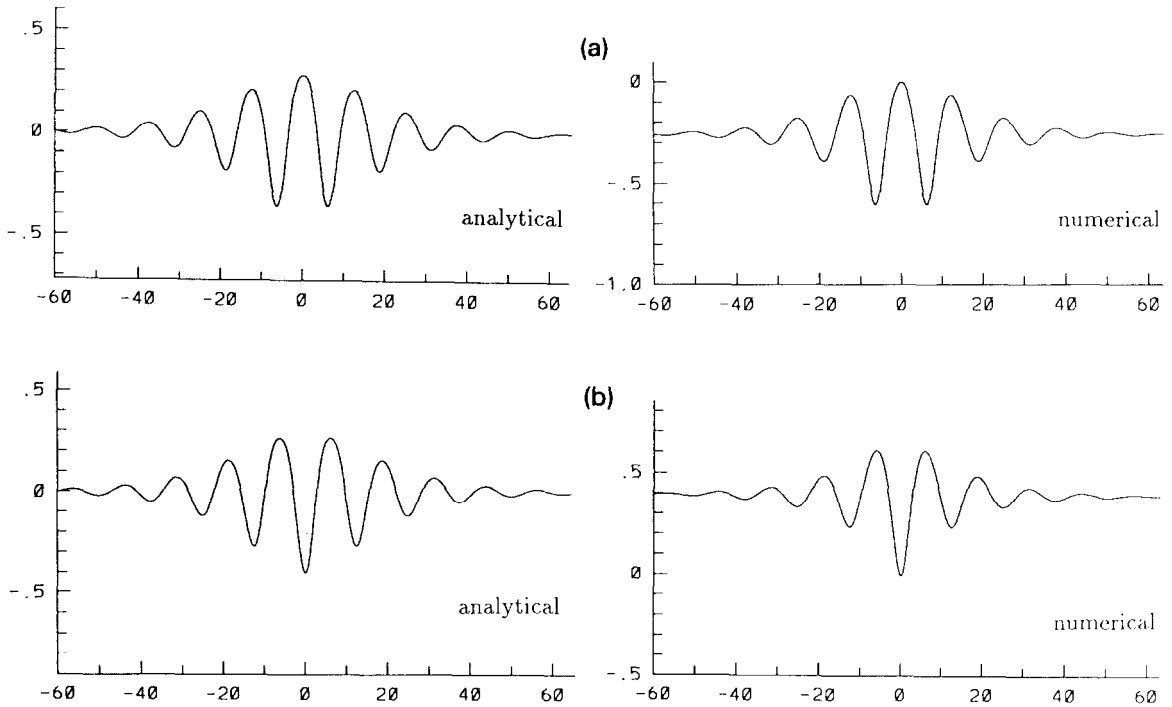


Fig. 6. Comparison between the wave profiles based on the formal limit of the analytical results as  $\kappa \rightarrow \infty$  and the numerical profile of Vanden-Broeck and Dias [6] for  $m = 0.005$ ; (a) elevation waves; (b) depression waves. Note that, in ref. [6], the elevation is chosen to be zero at  $x = 0$ .

Hunter and Vanden-Broeck [2] used a numerical scheme based on an integro-differential equation formulation to compute *depression* solitary waves with  $b < \frac{1}{3}$ . If one computes the values of  $\kappa$  and  $m$  corresponding to their profiles (see ref. [2], p. 200), one finds approximately (a)  $\kappa = 0.282$ ,  $m = 0.0101$ , (b)  $\kappa = 1.17$ ,  $m = 0.004$ , (c)  $\kappa = 1.59$ ,  $m = 0.0015$ . Since (a) and (b) are outside the range of validity of our analysis, we calculated the analytical profile corresponding to (c) and found a good agreement (see fig. 7). Since Hunter and Vanden-Broeck started from a value of  $b > \frac{1}{3}$  and decreased it below  $\frac{1}{3}$ , these results seem to indicate that the depression waves described in the present paper can be obtained continuously from the well-known solitary waves of depression with  $b > \frac{1}{3}$  (see for example Amick and Kirchgässner [7] and Sachs [8]).

Zufiria [3] developed a weakly nonlinear model for capillary-gravity waves with  $(b, \lambda)$  close to  $(\frac{1}{3}, 1)$ . He reduced the water-wave problem to a discrete Hamiltonian system of four first-order differential equations. Among its solutions, Zufiria found solitary waves, both of depression and elevation. His fig. 9, which has been reproduced in our fig. 8, shows approximations to such waves. These waves actually are periodic waves with a long wavelength of 100 times the depth. After reading the rough values of the physical parameters on Zufiria's fig. 8, we found the values of  $\kappa$  and  $m$  corresponding to these waves. After rescaling  $\eta$  and  $x$ , we plotted and compared the analytical profiles with Zufiria's profiles (see fig. 8). In view of the approximations involved in the comparison process and of the fact that the values of  $\kappa$  are "small," one can conclude that the agreement is rather good.

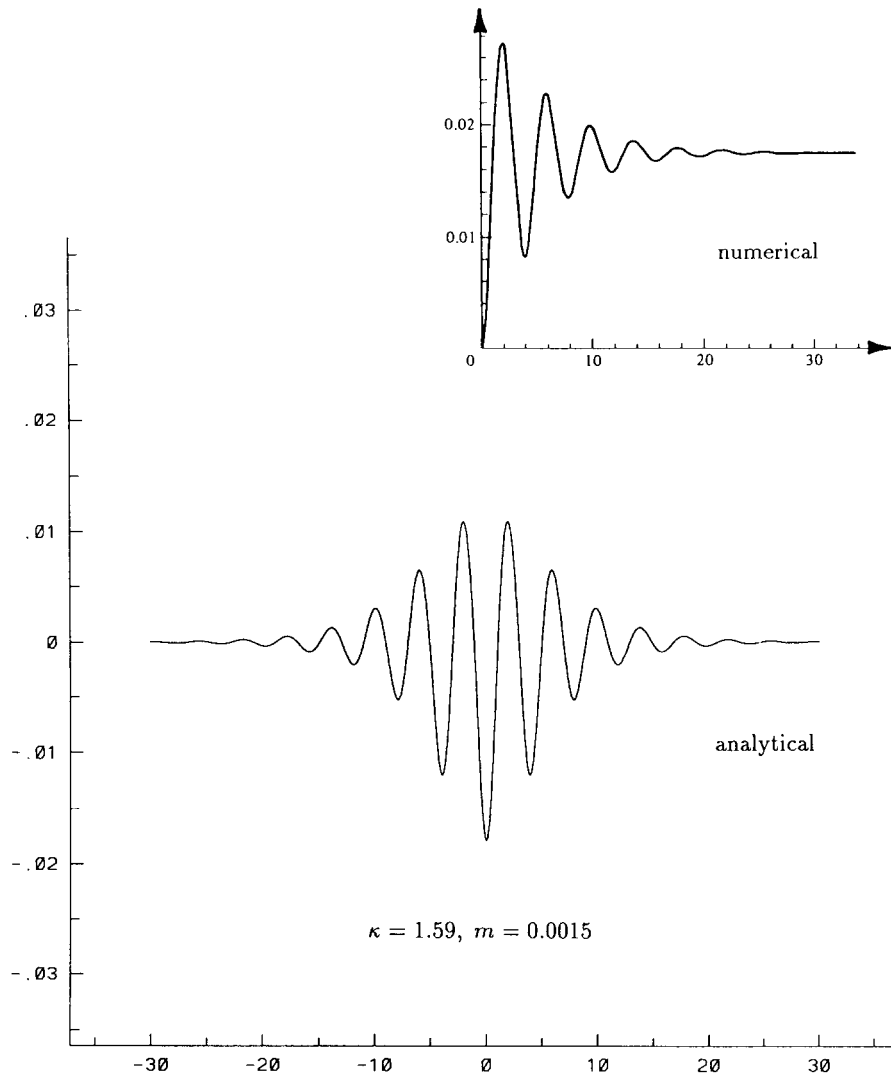


Fig. 7. Comparison between the analytical profile and the numerical profile of Hunter and Vanden-Broeck [2, fig. 4c, p. 215] for the depression wave with  $\kappa = 1.59$ ,  $m = 0.0015$ ,  $b = 0.2512$ ,  $\lambda = 1.0987$ . Note that, in Hunter and Vanden-Broeck, the elevation is chosen to be zero at  $x = 0$  and the unit length is the depth  $h$ . Since our unit length is  $bh$ , our profile has been rescaled accordingly.

As a conclusion, one might say that the analysis provides a good approximation of the solitary waves near the bifurcation curve. The bifurcation parameter we chose is  $m = b^*(\lambda - \lambda^*)$ , where the stars refer to the values given by eqs. (1.5) and (1.6). However, only the terms of orders  $\sqrt{m}$  and  $m$  were calculated in the analytical expansion and, as  $m$  increases, the terms of higher order might add a nonnegligible contribution. Numerical computations can complement the theoretical analysis by allowing to follow the branches of solutions away from the bifurcation curve. Numerical computations will also clarify how one can go continuously from the solitary waves of depression described in this paper to the well-known depression waves with  $b > \frac{1}{3}$ , and what happens to the waves of elevation as  $b$

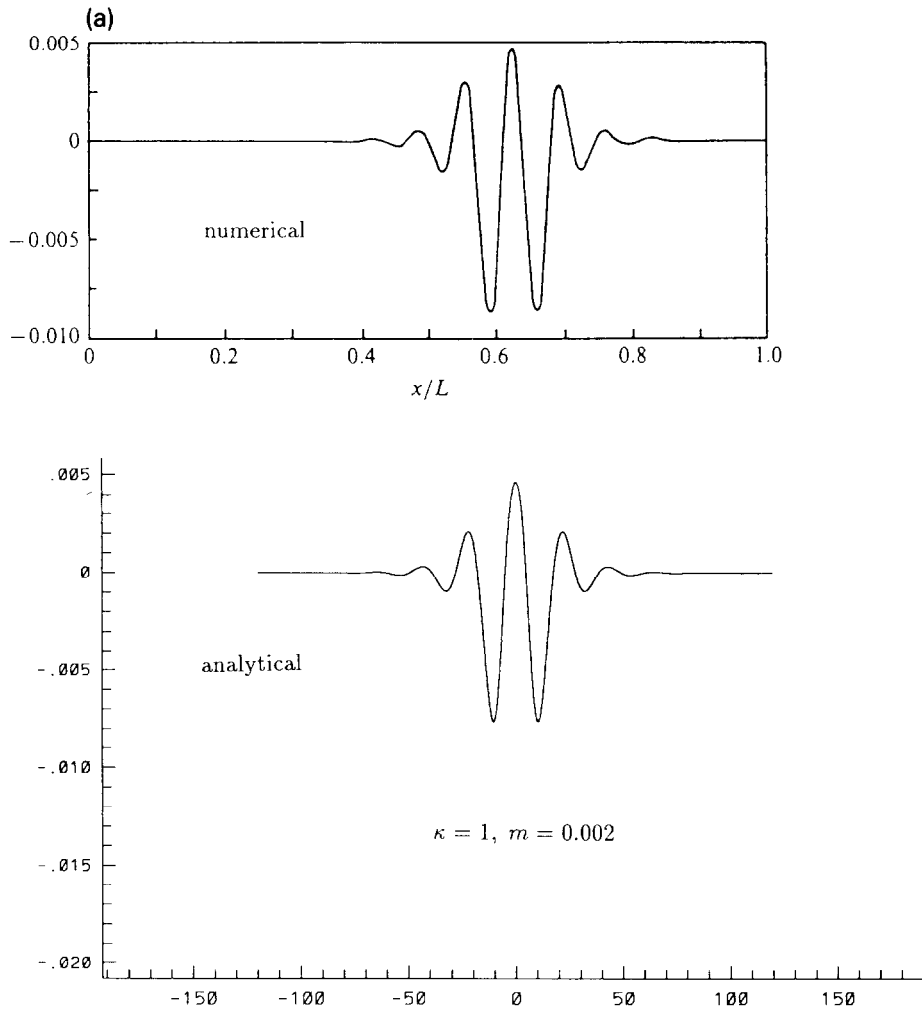


Fig. 8. Comparison between the analytical profiles and the numerical profiles of Zufiria [3, figs. 9a and 9b, p. 200]: (a) elevation wave with  $\kappa = 1$ ,  $m = 0.002$ ,  $b = 0.295$ ,  $\lambda = 1.025$ ; (b) depression wave with  $\kappa = 0.9$ ,  $m = 0.0013$ ,  $b = 0.301$ ,  $\lambda = 1.017$ . Note that Zufiria's waves actually are periodic waves with a very long wavelength  $L$ . Note also that Zufiria uses  $h$  as unit length. Our profiles have been rescaled accordingly.

is increased past  $\frac{1}{3}$ . Note that numerical computations near the bifurcation curve are hard because of the rapid oscillations and of the slow decay towards infinity.

### Acknowledgements

The authors are indebted to the referee who provided the reference to Kawahara's paper [1]. They would also like to thank Professor J.-M. Vanden-Broeck for valuable discussions on the topic of the present paper.

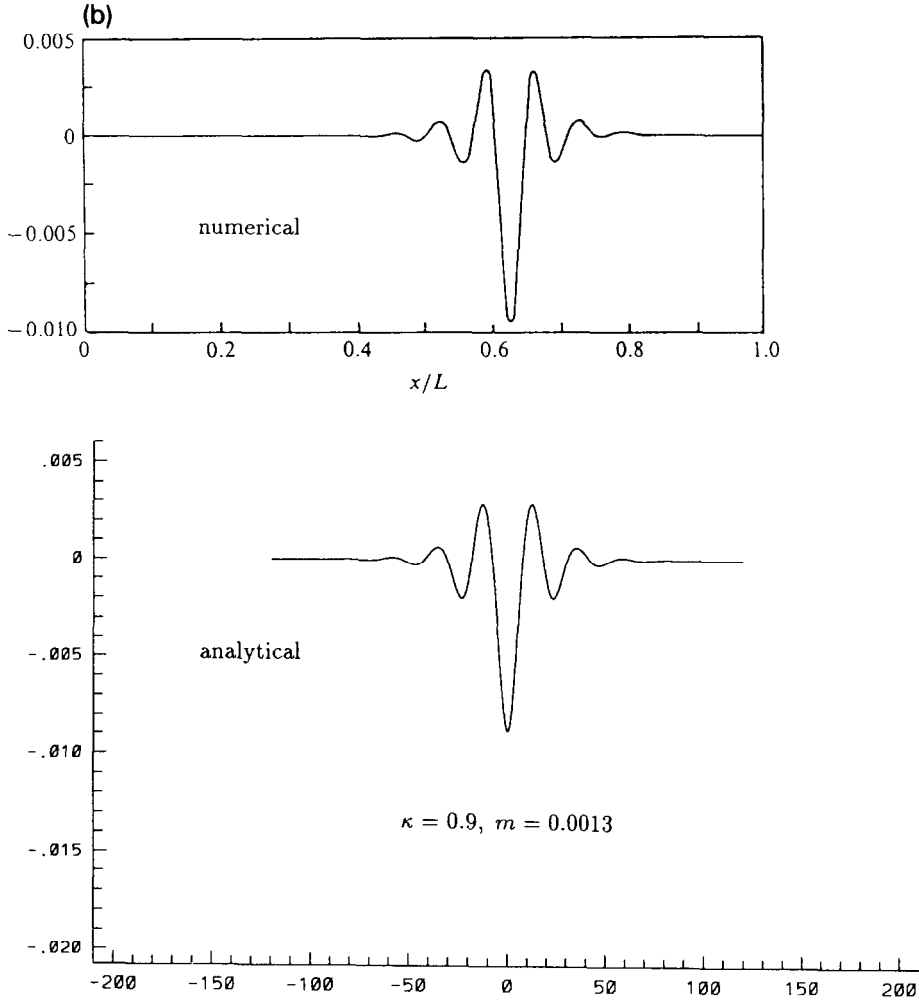


Fig. 8. (cont.).

## Appendix

In this appendix are given the vectors needed to compute the coefficients  $p_2$  and  $q_2$ . The computations are not difficult and consist in two major tasks: evaluating nonlinear terms (quadratic and cubic) given by (3.14) and (3.15) and integrating ordinary differential equations. In order to simplify the notation,  $\sinh \kappa$ ,  $\cosh \kappa$ ,  $\tanh \kappa$  are denoted by sh, ch, th below.

The vector  $\Phi_{2000}$  is obtained from (3.19) and is found to be

$$\Phi_{2000} = \begin{pmatrix} i(1 - \mathcal{A})\text{th} \\ \text{ch}^{-2} + \frac{1}{2}\mathcal{A}(\cosh 2k\psi + 2\text{th} \sinh 2k\psi + \text{th}^2 \cosh 2k\psi) \\ \frac{1}{2}i(1 - \mathcal{A})(\sinh 2k\psi + 2\text{th} \cosh 2k\psi + \text{th}^2 \sinh 2k\psi) \end{pmatrix}, \quad (\text{A.1})$$

where  $\mathcal{A}$  is a function of  $\kappa$  given by

$$\mathcal{A}(\kappa) = \frac{\text{sh}(5\text{ch}^2 + 4) - 3\kappa \text{ch}}{\text{sh}(\text{ch}^2 + 2) - 3\kappa \text{ch}}. \quad (\text{A.2})$$

The function  $\mathcal{A}$  is positive for all  $\kappa$  and the asymptotics are

$$\mathcal{A} \sim 5 \quad \text{as } \kappa \rightarrow \infty, \quad \mathcal{A} \sim 15\kappa^{-4} \quad \text{as } \kappa \rightarrow 0.$$

The vector  $\Phi_{1100}$  is obtained from (3.20) and is found to be

$$\Phi_{1100} = \begin{pmatrix} 0 \\ \frac{\lambda^*}{\lambda^* - 1} \left( \frac{1}{\text{ch}^2} + \frac{2\text{th}}{\kappa} \right) \\ 0 \end{pmatrix}. \quad (\text{A.3})$$

The vector  $\Phi_{1010}$  is obtained from (3.24) and is equal to

$$\Phi_{1010} = \begin{pmatrix} \frac{2\mathcal{B}\text{th}}{b} - \frac{1 - \mathcal{A}}{b \text{ch}^2} \\ \frac{i\mathcal{B} \cosh(2k\psi + 2\kappa)}{b \text{ch}^2} - \frac{i\mathcal{A}\psi \sinh(2k\psi + 2\kappa)}{\text{ch}^2} + \frac{2i}{b \text{sh ch}} + \frac{i\mathcal{A}}{b \text{ch}} \left( \frac{\cosh 2k\psi}{\text{sh}} - \frac{\sinh 2k\psi}{\text{ch}} \right) \\ \frac{\mathcal{B} \sinh(2k\psi + 2\kappa)}{b \text{ch}^2} + \frac{(1 - \mathcal{A})\psi \cosh(2k\psi + 2\kappa)}{\text{ch}^2} - \frac{1 - \mathcal{A}}{b \text{ch}} \left( \frac{\cosh 2k\psi}{\text{ch}} + \frac{\sinh 2k\psi}{\text{sh}} \right) \end{pmatrix}. \quad (\text{A.4})$$

The vector  $\Phi_{0110}$  is obtained from (3.25) and is equal to

$$\Phi_{0110} = \begin{pmatrix} -\frac{1}{b(\lambda^* - 1)} \left( \frac{1}{\text{ch}^2} + \frac{2\text{th}}{\kappa} \right) \\ \frac{i\lambda^*}{b\kappa^2(\lambda^* - 1)} \left( \text{th} + \frac{\kappa}{\text{ch}^2} + \frac{\kappa^2}{\text{sh ch}} \right) \\ -\frac{1}{\lambda^* - 1} \left( \psi + \frac{1}{b} \right) \left( \frac{1}{\text{ch}^2} + \frac{2\lambda^*\text{th}}{\kappa} \right) + \frac{\sinh(2k\psi + 2\kappa)}{b\kappa \text{ch}^2} \end{pmatrix}, \quad (\text{A.5})$$

where  $\mathcal{B}$  is a function of  $\kappa$  given by

$$\mathcal{B}(\kappa) = 3 \frac{\text{sh}^2 \text{ch}^2 (1 + 2\text{ch}^2) - 2\kappa \text{sh}^3 \text{ch} + (1 - 4\text{ch}^2) \kappa^2}{\kappa (\text{sh}(\text{ch}^2 + 2) - 3\kappa \text{ch})^2}. \quad (\text{A.6})$$

The function  $\mathcal{B}$  is positive for all  $\kappa$  and the asymptotics are

$$\mathcal{B} \sim 6\kappa^{-1} \quad \text{as } \kappa \rightarrow \infty, \quad \mathcal{B} \sim 40\kappa^{-5} \quad \text{as } \kappa \rightarrow 0.$$

The function  $\Phi$  in (3.6) commutes with the matrix  $R$  defined by (2.6). It follows that  $R\Phi_{2000} = \Phi_{0200}$ ,  $R\Phi_{1100} = \Phi_{1100}$ ,  $R\Phi_{0110} = -\Phi_{1001}$ ,  $R\Phi_{1010} = -\Phi_{0101}$ .



The coefficient  $q_2$  is obtained from (3.32) and is found to be

$$q_2(\kappa) = \frac{(\text{sh ch} - \kappa)^2}{8\text{sh}^2\text{ch}^2(\text{sh}^2\text{ch} + \kappa\text{sh} - 2\kappa^2\text{ch})(\kappa\text{sh ch} + \kappa^2 - 2\text{sh}^2)(\text{sh ch}^2 + 2\text{sh} - 3\kappa\text{ch})} \\ \times [9\kappa^4\text{sh ch} + 3\kappa^3(7\text{ch}^4 - 17\text{ch}^2 + 2) + \kappa^2\text{sh ch}(23\text{ch}^4 - 89\text{ch}^2 + 30) \\ + \kappa\text{sh}^2(11\text{ch}^6 - 37\text{ch}^4 + 58\text{ch}^2 + 4) - 2\text{sh}^3\text{ch}(3\text{ch}^4 - 13\text{ch}^2 - 2)].$$

The coefficient  $p_2$  is obtained from (3.31) and is found to be

$$p_2(\kappa) = \frac{\text{sh ch} - \kappa}{8\text{ch}^2(\text{sh}^2\text{ch} + \kappa\text{sh} - 2\kappa^2\text{ch})^2(\kappa\text{sh ch} + \kappa^2 - 2\text{sh}^2)(\text{sh ch}^2 + 2\text{sh} - 3\kappa\text{ch})^2} \\ \times [27\kappa^8\text{ch}^2(2\text{ch}^2 + 1) + 9\kappa^7\text{sh ch}(12\text{ch}^4 - \text{ch}^2 - 4) + 3\kappa^6(32\text{ch}^8 - 214\text{ch}^6 + 13\text{ch}^4 + 29\text{ch}^2 - 4) \\ + \kappa^5\text{sh}^3\text{ch}(20\text{ch}^6 - 346\text{ch}^4 - 31\text{ch}^2 + 24) \\ - \kappa^4\text{sh}^2(22\text{ch}^{10} - 93\text{ch}^8 - 707\text{ch}^6 - 808\text{ch}^4 - 42\text{ch}^2 + 8) \\ + \kappa^3\text{sh}^3\text{ch}(35\text{ch}^8 - 85\text{ch}^6 + 150\text{ch}^4 - 752\text{ch}^2 - 104) \\ - \kappa^2\text{sh}^4(127\text{ch}^8 + 149\text{ch}^6 + 792\text{ch}^4 - 64\text{ch}^2 - 32) \\ + \kappa\text{sh}^5\text{ch}(5\text{ch}^8 + 47\text{ch}^6 - 72\text{ch}^4 + 280\text{ch}^2 + 64) + 2\text{sh}^6\text{ch}^2(11\text{ch}^6 + 21\text{ch}^4 + 60\text{ch}^2 + 16)].$$

## References

- [1] T. Kawahara, Oscillatory solitary waves in dispersive media, *J. Phys. Soc. Jpn.* 33 (1972) 260.
- [2] J.K. Hunter and J.-M. Vanden-Broeck, Solitary and periodic gravity-capillary waves of finite amplitude, *J. Fluid Mech.* 134 (1983) 205.
- [3] J.A. Zufiria, Symmetry breaking in periodic and solitary gravity-capillary waves on water of finite depth, *J. Fluid Mech.* 184 (1987), 183.
- [4] M.S. Longuet-Higgins, Capillary-gravity waves of solitary type on deep water, *J. Fluid Mech.* 200 (1989) 451.
- [5] G. Iooss and K. Kirchgässner, Bifurcation d'ondes solitaires en présence d'une faible tension superficielle, *C.R. Acad. Sci. Paris* 311 I (1990) 265.
- [6] J.-M. Vanden-Broeck and F. Dias, Gravity-capillary solitary waves in water of infinite depth and related free surface flows, *J. Fluid Mech.* 240 (1992) 549.
- [7] C.J. Amick and K. Kirchgässner, A theory of solitary water-waves in the presence of surface tension, *Arch. Rational Mech. Anal.* 105 (1989) 1.
- [8] R.L. Sachs, On the existence of small amplitude solitary waves with strong surface tension, *J. Diff. Equ.* 90 (1991) 31.
- [9] G. Iooss and K. Kirchgässner, Water waves for small surface tension: an approach via normal form, *Proc. R. Soc. Edinburgh* 122A (1992) 267.
- [10] J.T. Beale, Exact solitary water waves with capillary ripples at infinity, *Commun. Pure Appl. Math.* 44 (1991), 211.
- [11] S.M. Sun, Existence of a generalized solitary wave solution for water with positive Bond number less than  $\frac{1}{3}$ , *J. Math. Anal. Appl.* 156 (1991) 471.
- [12] J.-M. Vanden-Broeck, Elevation solitary waves with surface tension, *Phys. Fluids A* 3 (1991) 2659.
- [13] E. Lombardi, Bifurcation d'ondes solitaires à oscillations de faible amplitude à l'infini, pour un nombre de Froude proche de 1, *C.R. Acad. Sci. Paris* 314 I (1992) 493.
- [14] A. Mielke, Reduction of quasilinear elliptic equations in cylindrical domains with applications, *Math. Meth. Appl. Sci.* 10 (1988) 51.
- [15] G. Iooss, A. Mielke and Y. Demay, Theory of steady Ginzburg-Landau equation, in hydrodynamic stability problems, *Eur. J. Mech. B/Fluids* 8 (1989) 229.
- [16] G. Iooss and M.-C. Pérouème, Perturbed homoclinic solutions in reversible 1:1 resonance vector fields, *J. Diff. Eq.*, to appear.
- [17] K. Kirchgässner, Nonlinearly resonant surface waves and homoclinic bifurcation, *Adv. Appl. Mech.* 26 (1988) 135.
- [18] G. Iooss and M. Adelmeyer, Topics in Bifurcation Theory and Applications, *Advanced Series in Nonlinear Dynamics* vol. 3 (World Scientific, Singapore, 1992).